J|A|C|S ARTICLES

Published on Web 12/23/2009

Design of Bis-spiropyran Ligands as Dipolar Molecule Receptors and Application to in Vivo Glutathione Fluorescent Probes

Na Shao,[†,⊥] Jianyu Jin,[†,‡] Hao Wang,[||] Jing Zheng,[‡] Ronghua Yang,*[,†,‡] Winghong Chan,*[,||] and Zeper Abliz[§]

Beijing National Laboratory for Molecular Sciences, College of Chemistry and Molecular Engineering, Peking University, Beijing, 100871, China, State Key Laboratory of Chemo/Biosensing and Chemometrics, College of Chemistry and Chemical Engineering, Hunan University, Changsha, 410082, China, Department of Chemistry, Hong Kong Baptist University, Kowloon Tong, Kowloon, Hong Kong, China, Institute of Materia Medica, Chinese Academy of Medical Science & Peking Union Medical College, Beijing, 100050, China, and College of Chemistry, Beijing Normal University, Beijing, 100875, China

Received September 27, 2009; E-mail: Yangrh@pku.edu.cn; Whchan@hkbu.edu.hk

Abstract: Despite considerable efforts toward the development of various sophisticated spiropyrans for metal ion sensing, less attention has been paid to organic molecule sensing. One of the major difficulties for detection of organic molecules using a spiropyran is the weak and nonspecific interaction between the spiropyran and the target. Here, we report the synthesis and molecular recognition characterization of two bis-spiropyrans for dipolar molecules and their application to in vivo glutathione (GSH) fluorescent probes. Unlike the mono-spiropyrans, the newly designed bis-spiropyran molecules feature a rigidly maintained molecular cleft and two spiropyran units as binding modules. The molecular recognition is based on multipoint electrostatic interactions and structure complementarity between the opened merocyanine form of the spiropyran and the analyte. It was observed that the spiropyran **1a** binds GSH in aqueous solution with high affinity ($K = (7.52 \pm 1.83) \times 10^4$ M^{-1}) and shows strong fluorescence emission upon binding. Remarkably, fluorescence output of **1a** is not significantly affected by other amino acids and peptides, especially, structurally similar compounds, such as cysteine and homocysteine. Furthermore, fluorescence anisotropy and confocal fluorescent microscopy confirmed that spiropyran **1a** is a comparatively good candidate for intracellular delivery and can be accumulated intensively into cells. Thus, **1a** can be utilized in vivo as a GSH probe or as a marker to show the level of intracellular GSH.

The construction of molecular-level devices with molecular recognition function and signal transduction ability is of great scientific interest and intense activity in the fields of chemistry,[1] biology,[2] sensors,[3,4] etc. Spiropyrans or spirobenzopyrans,[5] an important class of photochromic compounds, are an attractive starting point in such constructions because of their unique molecular binding ability and signal transduction function.[6] The photophysical property of a spiropyran is sensitive to surrounding media, displaying reversible structural transformation from the closed spiropyran (spiro) form to the opened merocyanine (mero) form upon thermal or light stimuli, and external substrate complexation.[7] The exploitation of such characteristics in spiropyrans has led to development of molecular switches in materials chemistry[6] and also molecular sensors in analytical

[†] Peking University.
[‡] Hunan University.
[||] Hong Kong Baptist University.
[§] Chinese Academy of Medical Science & Peking Union Medical College.
[⊥] Present address: Beijing Normal University.

(1) (a) Valeur, B.; Badaoui, F.; Bardez, E.; Bourson, J.; Boutin, P.; Chatelain, A.; Devol, I.; Larrey, B.; Lefevre, J. P.; Soulet, A. In *Chemosensors of Ion and Molecule Recognition*; Desvergne, J.-P., Czarnik, A. W., Eds.; NATO ASI Series, Series C: Vol. 492; Kluwer Academic Press: Dordrecht, The Netherlands, 1997. (b) de Silva, A. P.; Gunaratne, H. Q. N.; Gunnlaugsson, T.; Huxley, A. J. M.; McCoy, C. P.; Rademacher, J. T.; Rice, T. E. *Chem. Rev.* **1997**, *97*, 1515–1566. (c) Pu, L. *Chem. Rev.* **2004**, *104*, 1687–1716. (d) Filippini, D.; Alimelli, A.; Di Natale, C.; Paolesse, R.; D'Amico, A.; Lundstrom, I. *Angew. Chem., Int. Ed.* **2006**, *45*, 3800–3803.
(2) (a) Gonçalves, M. S. T. *Chem. Rev.* **2009**, *109*, 190–212. (b) Liu, J. W.; Cao, Z. H.; Lu, Y. *Chem. Rev.* **2009**, *109*, 1948–1998.
(3) Borisov, S. M.; Wolfbeis, O. S. *Chem. Rev.* **2008**, *108*, 423–461.
(4) (a) Wang, L. Y.; Yan, R. X.; Hao, Z. Y.; Wang, L.; Zeng, J. H.; Bao, H.; Wang, X.; Peng, Q.; Li, Y. D. *Angew. Chem., Int. Ed.* **2005**, *44*, 6054–6057. (b) Liu, J. W.; Lu, Y. *Angew. Chem., Int. Ed.* **2006**, *45*, 90–94.
(5) The IUPAC nomenclature of spiropyran is 1′,3′-dihydro-1′,3′,3′-trimethyl-spiro-[2*H*-1-benzopyran-2,2′-indoline].
(6) For reviews, see (a) Bertelson, R. C. In *Photochromism*; Brown, G. H.; Ed.; Wiley Interscience: New York, 1971; pp 45−431, and references therein. (b) Guglielmetti, R. In *Photochromoism: Molecules and Systems, Studies in Organic Chemistry*; Dürr, H.; Bouas-Laurent, H., Eds.; Elsevier: Amsterdam, 1990,Chapter 8 and 23, and references therein. (c) Berkovic, G.; Krongauz, V.; Weiss, V. *Chem. Rev.* **2000**, *100*, 1741–1753. (d) Minkin, V. I. *Chem. Rev.* **2004**, *104*, 2751–2776.
(7) (a) Fischer, E.; Hirshberg, Y. *J. Chem. Soc.* **1952**, 4522–4524. (b) Day, J. H. *Chem. Rev.* **1963**, *63*, 65–80. (c) Taylor, L. D.; Nicholson, J.; Davis, R. B. *Tetrahedron Lett.* **1967**, *8*, 1585–1588. (d) Byrne, R.; Kevin, J.; Fraser, K. J.; Izgorodin, E.; MacFarlane, D. R.; Forsyth, M.; Diamond, D. *Phys. Chem. Chem. Phys.* **2008**, *10*, 5919–5924.

Scheme 1. Comparison of the Possible Schemes of the Photochemical Ring-Opening of Mono-spiropyran **2** (A) and Bis-spiropyran **1a** (B and C) in the Presence of GSH and Cys

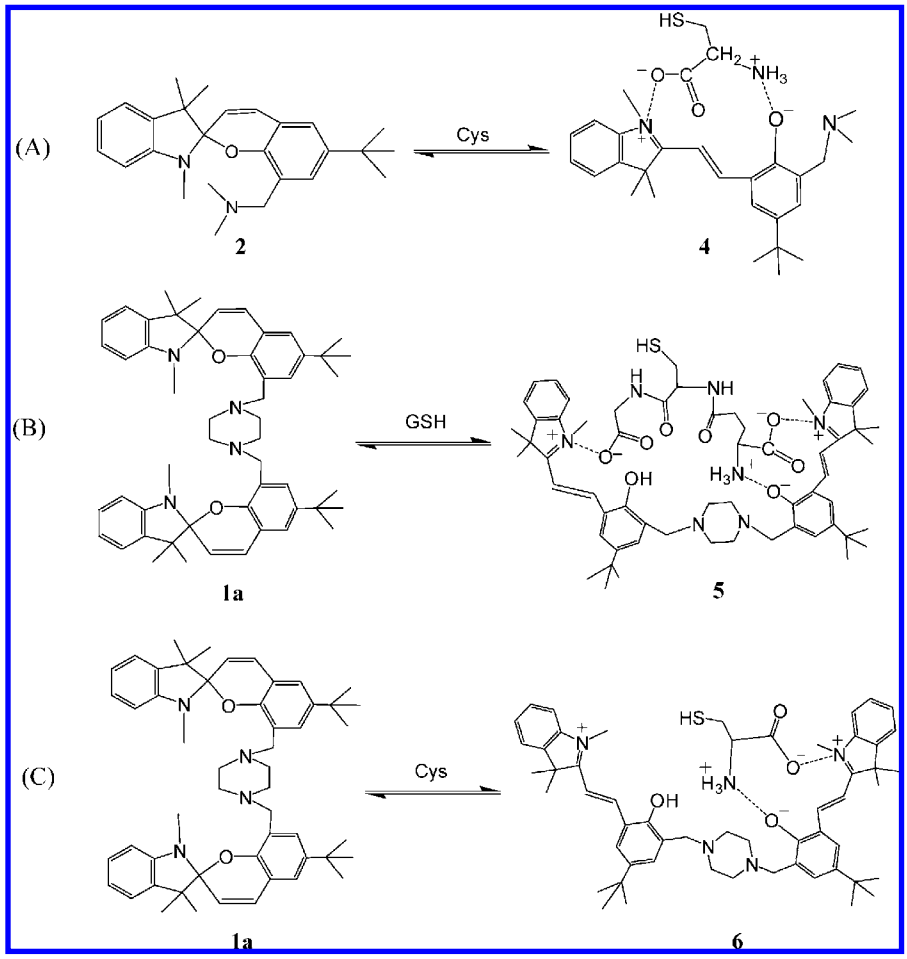

chemistry.[8] During recent decades, a number of receptors possessing diverse spiropyran skeletons have been designed and utilized for optical sensing of metal ions.[8−11] In contrast, only a few examples for the sensing of anions[12] and organic molecules[13−15] have been reported.

Pioneered by the seminal work of Sunamoto et al.[16] as early as 1982, it has been demonstrated that the zwitterionic mero form of a spiropyran can bind a polar amino acid molecule via electrostatic interaction (Scheme 1A), making spiropyrans attractive materials for photocontrolled transfer of amino acid derivatives across bilayers[16] or as capture agents for amino acids on the surface of gold nanoparticles.[17] However, in view of the molecular design, all these approaches were limited to one spiropyran unit to interact with the target. Drawbacks toward a practical sensor for selective detection of a particular analyte exist: first, for a mono-spiropyran receptor, only one additional interaction is available for binding when the spiropyran unit is opened, which would lead to low affinity for the target molecule.

(8) For two reviews, see: (a) Inouye, M. *Coord. Chem. Rev.* **1996**, *148*, 265–283. (b) Byrne, R.; Diamond, D. *Nat. Mater.* **2006**, *5*, 421–426.
(9) For spiropyran-based fluorescent probes for metal ions, see: (a) Preigh, M. J.; Lin, F. T.; Ismail, K. Z.; Weber, S. G. *J. Chem. Soc., Chem. Commun.* **1995**, 2091–2092. (b) Winkler, J. D.; Bowen, C. M.; Michelet, V. *J. Am. Chem. Soc.* **1998**, *120*, 3237–3242. (c) Shao, N.; Zhang, Y.; Cheung, S.; Yang, R. H.; Chan, W. H.; Mo, T.; Li, K. A.; Liu, F. *Anal. Chem.* **2005**, *77*, 7294–7303. (d) Shao, N.; Jin, J. Y.; Wang, H.; Zhang, Y.; Yang, R. H.; Chan, W. H. *Anal. Chem.* **2008**, *80*, 3466–3475.
(10) For examples for spiropyran-based colorimetric probes for heavy- or transition- metal ions, see: (a) Chibisov, A. K.; Gorner, H. *Chem. Phys.* **1998**, *237*, 425–442. (b) Gorner, H.; Chibisov, A. K. *J. Chem. Soc., Faraday Trans.* **1998**, *94*, 2557–2564. (c) Evans, L.; Collins, G. E.; Shaffer, R. E.; Michelet, V.; Winkler, J. D. *Anal. Chem.* **1999**, *71*, 5322–5327. (d) Collins, G. E.; Choi, L. S.; Ewing, K. J.; Michelet, V.; Bowen, C. M.; Winkler, J. D. *Chem. Commun.* **1999**, 321–322. (e) Nishikiori, H.; Sasai, R.; Arai, N.; Arai, N.; Takagi, K. *Chem. Lett.* **2000**, 1142–1143. (f) Leaustic, A.; Dupont, A.; Yu, P.; Clement, R. *New J. Chem.* **2001**, *25*, 1297–1301. (g) Wojtyk, J. T. C.; Kazmaier, P. M.; Buncel, E. *Chem. Mater.* **2001**, *13*, 2547–2551. (h) Kopelman, R. A.; Snyder, S. M.; Frank, N. L. *J. Am. Chem. Soc.* **2003**, *125*, 13684–13685.
(11) For examples for spiropyran-based colorimetric probes for alkali- or alkaline- metal ions, see: (a) Kimura, K.; Yamashita, T.; Yokoyama, M. *J. Chem. Soc., Chem. Commun.* **1991**, 147–148. (b) Kimura, K.; Kaneshige, M.; Yamashita, T.; Yokoyama, M. *J. Org. Chem.* **1994**, *59*, 1251–1256. (c) Kimura, K.; Utsumi, T.; Teranishi, T.; Yokoyama, M.; Sakamoto, H.; Okamoto, M.; Arakawa, R.; Moriguchi, H.; Miyaji, Y. *Angew. Chem., Int. Ed. Engl.* **1997**, *36*, 2452–2454. (d) Salhin, A. M. A.; Tanaka, M.; Kamada, K.; Ando, H.; Ikeda, T.; Shibutani, Y.; Yajima, S.; Nakamura, M.; Kimura, K. *Eur. J. Org. Chem.* **2002**, 655–662. (e) Yai, S.; Nakamura, S.; Watanabe, D.; Nakazumi, H. *Dyes Pigm.* **2009**, *80*, 98–105.
(12) Shiraishi, Y.; Adachi, K.; Itoh, M.; Hirai, T. *Org. Lett.* **2009**, *11*, 3482–3485.
(13) Inouy, M.; Kim, K.; Kito, T. *J. Am. Chem. Soc.* **1992**, *114*, 778–780.
(14) (a) Tsubaki, K.; Mukoyoshi, K.; Morikawa, H.; Kinoshita, T.; Fuji, K. *Chirality* **2002**, *14*, 713–715. (b) Liu, Y. Y.; Fan, M. G.; Zhang, S. X.; Sheng, X. H.; Yao, J. N. *New J. Chem.* **2007**, *31*, 1878–1881.
(15) Shao, N.; Jin, J. Y.; Cheung, S. M.; Yang, R. H.; Chan, W. H.; Mo, T. *Angew. Chem., Int. Ed.* **2006**, *45*, 4944–4948.
(16) Sunamoto, J.; Iwamoto, K.; Mohri, Y.; Kominato, T. *J. Am. Chem. Soc.* **1982**, *104*, 5502–5504.
(17) Ipe, B. I.; Mahima, S.; Thomas, K. G. *J. Am. Chem. Soc.* **2003**, *125*, 7174–7175.

Chart 1. Molecular Structures of the Spiropyran Probes of **1a**, **1b**, and **2**, and the Analytes of **3a** (GSH), **3b**, and **3c** Examined in This Work

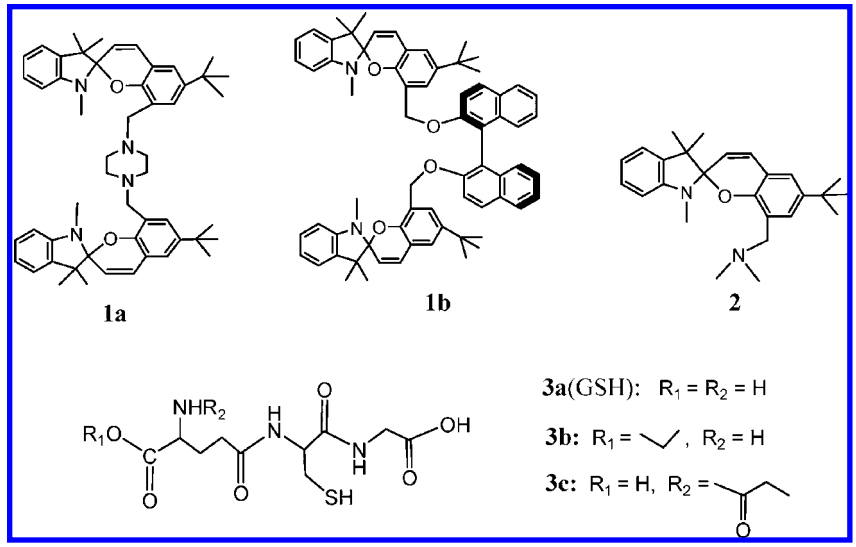

Furthermore, electrostatic interactions are nondirectional, and, as a result, all polar charged molecules are attracted to such a receptor.

Therefore, we are interested in developing a highly sensitive and selective spiropyran-based probe for organic molecules. The issue of affinity and selectivity could be addressed by the use of cooperative recognition.[18,19,15] In fact, for selective detection of metal ions, various sophisticated spiropyrans with multiple binding sites in the molecular backbone have been developed.[11] To the best of our knowledge, however, no work has, so far, been reported regarding selectivity and sensitivity for organic molecules utilizing the structural variants of spiropyran, even though it is well-known that the weak and nonspecific host−guest interaction is the major difficulty for this approach. Here, we present the rational design of two bis-spiropyran dyads, **1a** and **1b** (Chart 1), and the study of their molecular recognition features for complementary charged molecules. Notably, **1a** exhibited a highly selective response toward reduced glutathione (GSH) through significant color change and fluorescence emission enhancement of the probe. Moreover, cell experiments indicated that **1a** is membrane-permeable due to the moderately high hydrophobicity. Confocal fluorescence microscopy experiments established that **1a** is GSH-responsive in vivo and produces fluorescence enhancement in living cells by GSH complexation.

GSH (γ-glutamyl-cysteinyl-glycine) is the most abundant cellular thiol compound[20] and is involved in many important functions in the body including the control of the redox environment in cells.[21] Analysis of GSH is of continuous interest because of its biological and clinical significance. The commonly used methods for the determination of GSH are based on redox chemistry or labeling with chromophores or fluorophores through the combination of chromatographic separation and spectroscopic detection.[22,23] The derivation methods, however, suffer from various disadvantages such as being time-consuming, having poor sensitivity, and requiring a large sample amount. Since there is an increasing demand for real-time monitoring of GSH during biotechnical processes, the construction of functional approaches that could quickly and reversibly recognize and detect the analyte is of current interest and is highly required.[24] Toward this goal, various molecular probes, using organic small molecules,[25−34] metal complexes,[35,36] gold nanorods,[37] and quantum dots,[38] have been developed for GSH and thiol-containing amino acids. Although these approaches have led to significant contributions to the GSH assay, we noted that the molecular recognition step of the approaches is based on interactions of the SH of the analyte and the probe molecules through covalent chemical reactions[25−29,31−33] or metal coordinations.[35−38] Such reactions are irreversible and are not fast enough to allow real-time detection under physiological conditions. Furthermore, discrimination of GSH from sulfhydryl-containing amino acids and peptides is hampered because of interference from these structurally related molecules. Therefore, it is desirable to develop a new method to alleviate these problems

(18) Ercolani, G. *J. Am. Chem. Soc.* **2003**, *125*, 16097–160103.
(19) Aït-Haddon, H.; Wishur, S. L.; Lynch, V. M.; Anslyn, E. V. *J. Am. Chem. Soc.* **2001**, *123*, 11296–11297.
(20) (a) Meister, A.; Anderson, M. E. *Annu. Rev. Biochem.* **1983**, *52*, 711–760. (b) Anderson, M. E. *Chem.-Biol. Interact.* **1998**, *112*, 1–14.
(21) (a) Smith, C. V.; Jones, D. P.; Guenthner, T. M.; Lash, L. H.; Lauterburg, B. H. *Toxicol. Appl. Pharmacol.* **1996**, *140*, 1–12. (b) Schafer, F. Q.; Buettner, G. R. *Free Radical Biol. Med.* **2001**, *30*, 1191–1212.
(22) (a) Pastore, A.; Federici, G.; Bertini, E.; Piemonte, F. *Clin. Chim. Acta* **2003**, *333*, 19–39. (b) Camera, E.; Picardo, M. *J. Chromatogr. B* **2002**, *781*, 181–206.
(23) (a) Mansoor, M. A.; Svardal, A. M.; Ueland, P. M. *Anal. Biochem.* **1992**, *200*, 218–229. (b) Rossi, R.; Milzani, A.; Dalle-Donne, I.; Giustarini, D.; Lusini, L.; Colombo, R.; Di Simplicio, P. *Clin. Chem.* **2002**, *48*, 742–753. (c) Nèmeth-Kiss, V.; Forgács, E.; Cserháti, T. *J. Chromatogr. A* **1997**, *776*, 147–152. (d) Sakhi, A. K.; Russnes, K. M.; Smeland, S.; Blomhoff, R.; Gundersen, T. E. *J. Chromatogr. A* **2006**, *1104*, 179–189.
(24) (a) Nekrrassova, O.; Lawrence, N. S.; Compton, R. G. *Talanta* **2003**, *60*, 1085–1095. (b) Haugland, R. P. *Handbook of Fluorescent Probes and Research Products*, 9th ed.; Molecular Probes, Inc.: Eugene, OR, 2002; pp 79−98.
(25) (a) Rusin, O.; St Luce, N. N.; Agbaria, R. A.; Escobedo, J. O.; Jiang, S.; Warner, I. M.; Dawan, F. B.; Lian, K.; Strongin, R. M. *J. Am. Chem. Soc.* **2004**, *126*, 438–439. (b) Wang, W. H.; Escobedo, J. O.; Lawrence, C. M.; Strongin, R. M. *J. Am. Chem. Soc.* **2004**, *126*, 3400–3401. (c) Wang, W.; Rusin, O.; Xu, X.; Kim, K. K.; Escobedo, J. O.; Fakayode, S. O.; Fletcher, K. A.; Lowry, M.; Schowalter, C. M.; Lawrence, C. M.; Fronczek, F. R.; Warner, I. M.; Strongin, R. M. *J. Am. Chem. Soc.* **2005**, *127*, 15949–15958, and references therein.
(26) Yi, L.; Li, H. Y.; Liu, L. L.; Zhang, C. H.; Xi, Z. *Angew. Chem., Int. Ed.* **2009**, *48*, 4034–4037.
(27) Maeda, H.; Matsuno, H.; Ushida, M.; Katayama, K.; Saeki, K.; Itoh, N. *Angew. Chem., Int. Ed.* **2005**, *44*, 2922–2925.

Scheme 2. Preparation of Bis-spiropyrans **1a** and **1b**

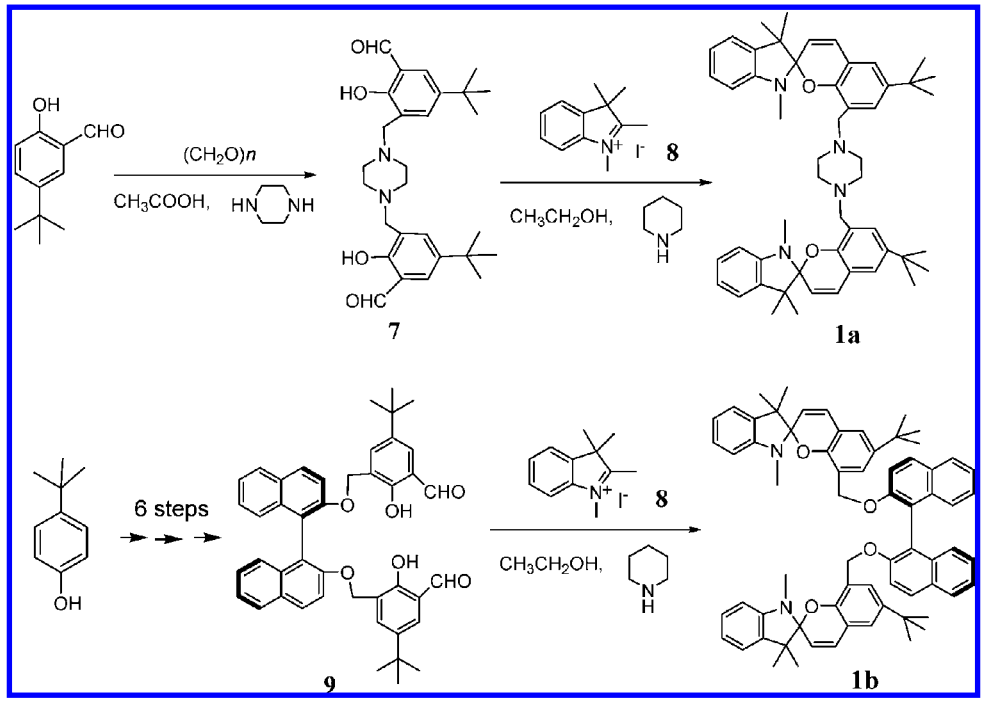

and, more importantly, to allow its direct analysis in vivo.[26,30] This approach requires the integration of capabilities for cell permeability, selective recognition in vivo of the target stimulus, and generation of detectable signals.

Results and Discussion

Probe Design and Synthesis. Chart 1 shows the molecular structures of **1a** and **1b**. The choice of the recognition element was guided by the considerations of the high affinity and specificity to the target. In previous literature, it was proven that the zwitterionic merocyanine of a spiropyran could bind a polar amino acid molecule via electrostatic interaction.[16] First, to achieve strong and highly specific binding to dipolar molecules, the receptor domains of **1a** and **1b** were formed by introducing two spiropyran units which are assembled as a binding module, and a piperazine or binol moiety, respectively, as a linking spacer. Unlike the mono-spiropyrans, **1a** and **1b** feature a rigidly maintained molecular cleft and two zwitterionic merocyanine units into which a molecule of suitable size, shape, and multipoint bonding capacity is expected to be more effectively bound. This design would provide a reasonable system in terms of sensitivity and selectivity. Second, to ensure that the probes can function without light protection, an electron-rich group, *tert*-butyl, was introduced in the 6′-position, superseding the electron-withdrawing nitro group, to obtain a stable optical signal without photochromic behavior upon ultraviolet light irradiation. Finally, the introduction of an alkylated chain in the molecular skeleton assures moderately high hydrophobicity of the material, which meets the requirement to diffuse across cell membranes for an in vivo assay.

The synthesis of bis-spiropyrans **1a** and **1b** is shown in Scheme 2. Linking two hydroxybenzaldehyde moieties by a Mannich-type reaction of piperazine and formaldehyde was accomplished readily in acetic acid, giving rise to the bis-adduct **7** in 62% yield. On the other hand, according to the recent synthetic work by Maria et al.,[39] precursor **9** was assembled from 4-*tert*-butylphenol in a six-step reaction sequence. To complete the synthesis, the condensation reaction of bis-phenol **7** or **9** with 2 equiv of *N*-methyl-2,3,2-trimethylindolenine (**8**) in the presence of piperidine affords **1a** or **1b** in 49% and 87% yield, respectively.

Photophysical Properties of 1a and 1b in Aqueous Solution. Table 1 summarizes the photophysical parameters of **1a** and **1b** at room temperature. The photophysical property of a spiropyran is related to the chemical structure of the spiropyran unit and surrounding media, such as the solvent polarity and the external substrate complexation.[6] Both **1a** and **1b** are soluble in DMSO, ethanol, and CH_2Cl_2, etc. Although **1a** and **1b** are insoluble in water, their solubility in the ethanol−water system is good. If the probes were first dissolved in ethanol, and water was then added, a clear homogeneous aqueous solution can be formed in 90% (v/v) water−ethanol if the concentration of the probes is low. This relatively high solubility is due to the formation of few polar mero-components of the probes induced

(28) Fujkawa, Y.; Urano, Y.; Komatsu, T.; Hanaoka, K.; Kojima, H.; Terai, T.; Inoue, H.; Nahano, T. *J. Am. Chem. Soc.* **2008**, *130*, 14533–14543.
(29) Ros-Lis, J. V.; Garcâa, B.; Jiménez, D.; Martânez-Máñez, R.; Sancenón, F.; Soto, J.; Gonzalvo, F.; Valldecabres, M. C. *J. Am. Chem. Soc.* **2004**, *126*, 4064–4065.
(30) Ahn, Y. H.; Lee, J. S.; Chang, Y. T. *J. Am. Chem. Soc.* **2007**, *129*, 4510–4511.
(31) Julia Guy, J.; Caron, K.; Dufresne, S.; Michnick, S. W.; Skene, W. G.; Jeffrey, J. W. *J. Am. Chem. Soc.* **2007**, *129*, 11969–11977.
(32) Novak, M.; Lin, J. *J. Am. Chem. Soc.* **1996**, *118*, 1302–1308.
(33) Jing, W.; Fu, Q.; Fan, H.; Ho, J.; Wang, W. *Angew. Chem., Int. Ed.* **2007**, *46*, 8445–8448.
(34) Matsumoto, T.; Urano, Y.; Shoda, T.; Kojima, H.; Nagano, T. *Org. Lett.* **2007**, *9*, 3375–3377.
(35) Chow, C. F.; Chiu, B. K. W.; Lam, M. H. W.; Wong, W. Y. *J. Am. Chem. Soc.* **2003**, *125*, 7802–7803.
(36) Han, S. M.; Kim, D. H. *Tetrahedron* **2004**, *60*, 11251–11257.
(37) Sudeep, P. K.; Joseph, S. T.; Thomas, K. G. *J. Am. Chem. Soc.* **2005**, *127*, 6516–6517.
(38) Han, B. Y.; Yuan, J. P.; Wang, E. K. *Anal. Chem.* **2009**, *81*, 5569–5573.
(39) Maria, E. A.; Francesco, P. B.; Andrea, P.; Domenico, S.; Gaetano, A. T.; Rosa, M. T. *Tetrahedron.* **2007**, *63*, 9751–9757.

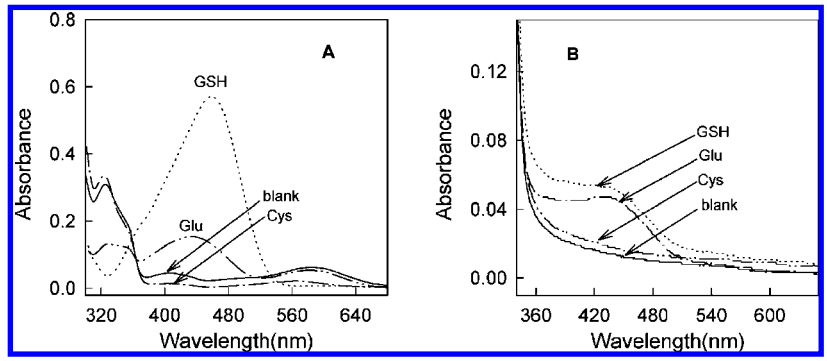

Figure 1. Absorption spectral changes of **1a** (A) and **1b** (B) recorded in 20% ethanol−water solution in the presence of 0.5 mM Cys, Glu, and GSH, separately. The concentrations of **1a** and **1b** are each 5.0×10^{-5} M.

Table 1. Photophysical Properties of **1a** and **1b** and Their GSH Complexes in 20% Ethanol−Water Solution at pH 7.2 at Room Temperature

	absorption		emission		
	λ_{max} (nm)	ε_{max} (cm^{-1}, M^{-1})	λ_{max} (nm)	Φ	$\langle\tau\rangle$ (ns)
1a	334	2.04×10^4	516	0.08	4.01
	587	4.37×10^2	−	−	−
1a−GSH[a]	446	5.28×10^4	643	0.61	5.03
1b	321	1.21×10^4	560	0.13	4.96
1b−GSH[a]	430	2.69×10^4	590	0.05	4.52

[a] The concentration of GSH was 1.0×10^{-3} M.

by water. To ensure that the spiropyrans are completely dissolved, the 20% ethanol−water system was employed to investigate the photochromic behavior of **1a** and **1b** in aqueous solution.

In ethanol−water solution, both **1a** and **1b** are colorless and display maximum absorption wavelengths at 334 and 321 nm, respectively. Irradiation of the spiropyran solutions with UV light caused no significant differences in the absorption spectra,[40] reflecting the nearly complete absence of the mero-component. These observations are distinctly different from the photochromic property of the common 6′-nitro-substituted mono-spiropyrans, which are strongly photochromic in polar solvents. This difference could be attributed to the electronic effects of the substituent as previously demonstrated.[41,42]

Another extremely important factor for changing the photophysical properties of spiropyran is complexation-modulation. The complexation of external substrates with the opened merocyanine is favorable for conversion of the spiro-form to the mero-form. To test the capability of complexation-induced ring-opening of **1a** or **1b**, we first investigated the effects of three dipolar molecules, cysteine (Cys), glutamic acid (Glu), and GSH, on the UV−visible absorption spectra of the spiropyrans in ethanol−water solution. Figure 1 shows the absorption spectral changes of the two spiropyrans upon addition of 0.5 mM Cys, Glu, and GSH, separately. As expected, **1a** shows different absorption response behaviors to the complementary charged molecules of different structures. In the presence of Cys, **1a** does not exhibit significant absorption spectral change, while for addition of Glu, slight absorption enhancement is observed in the visible range but the color of the solution remains colorless. However, upon addition of GSH to the ethanol−water solution, **1a** evidently displays a strong absorption enhancement at 446 nm concomitant with a change of the solution color from colorless into yellow, reflecting complete formation of the opened mero-form. As for **1b**, the absorption at 450 nm was slightly enhanced by Glu or GSH under the same conditions (Figure 1B). The phenomena demonstrate that, in a given medium, the photophysical property of a spiropyran is dependent on the nature of both the host and guest molecules. The different photochromic behaviors of **1a** induced by the structurally similar analytes, Cys and GSH, indicate that structural complementarity of host−guest is the key factor for the binding interaction. Scheme 1 shows the molecular structure models of **1a** with Cys and GSH which was energy-minimized using Chemoffice 7.0 MM2 utilities. The suitable size, shape, and multipoint bonding capacity of GSH with **1a** are expected to be more effective for binding than that of Cys.

Figure 2A shows the absorption changes of **1a** upon addition of an increasing concentration of GSH. The ligand-free **1a** shows a prominent band at 334 nm corresponding to the spiropyran form. The additional weak absorption at 490−650 nm is ascribed to the slightly protonated merocyanine component. Addition of increasing amounts of GSH to the ethanol−water solution of **1a** leads to strong absorption at 446 nm with a decrease in the absorbance of the two intrinsic bands accompanied by two isosbestic points at 345 and 528 nm, respectively. The absorbance at 446 nm increases considerably as the GSH concentration is increased, approximately up to 50 equiv relative to the host concentration. Further increase in the GSH concentration leads to a slight increase in the absorption at the wavelength. These spectroscopic changes are characteristic of spiropyran when a complexation process is accompanied by ring-opening. In aqueous solution, there is equilibrium initially between spiropyran and a minor amount of protonated merocyanine as indicated by the weak absorption in the visible region, and complexation of GSH with merocyanine drives the equilibrium toward the mero-GSH form, leading to disappearance of the intrinsic absorption band and appearance of a new absorption in the visible region.

The fluorescence emission of **1a** is also sensitive to the presence of GSH. Recent investigations on the fluorescence properties of spiropyran-based systems indicate that the closed spiro-form has no emission, while the zwitterionic mero-form emits at around 650 nm.[9b] When excited at the maximum absorption wavelength, **1a** fluoresces with its maximum emission wavelength at 516 nm ($\Phi_F = 0.08$), but no fluorescence emission in the red region of 600−700 nm could be measured,

(40) For details, see Supporting Information.
(41) Keum, S.-R.; Lee, K.-B.; Kazmaier, P. M.; Buncel, E. *Tetrahedron Lett.* **1994**, *35*, 1015–1018.
(42) Swansburg, S.; Bucel, E.; Lemieux, R. P. *J. Am. Chem. Soc.* **2000**, *122*, 6594–6600.

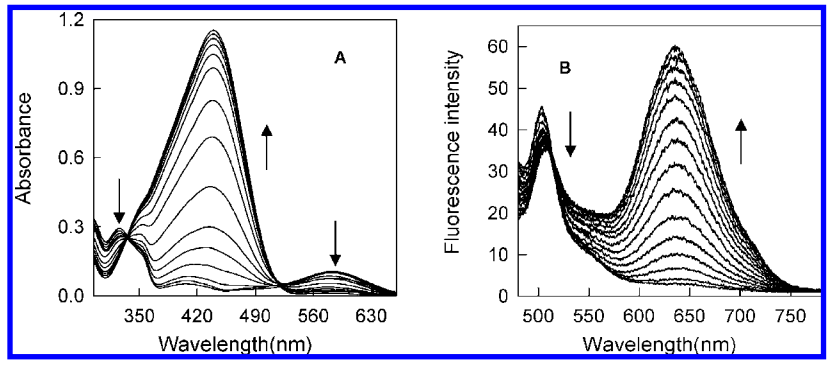

Figure 2. Absorption (A) and fluorescence emission (B, λ_{ex} = 446 nm) spectra of **1a** recorded in 20% ethanol−water solution in the presence of an increasing concentration of GSH. Aliquots of 0.05, 1.0, and 50 mM GSH stock solutions were added to afford 0, 0.005, 0.01, 0.025, 0.05, 0.1, 0.15, 0.3, 0.5, 0.75, 1.0, 1.5, 2.0, 3.0, and 5.0 mM GSH.

Table 2. Fluorescence Decay Data of **1a** (1.0×10^{-4} M) in the Absence and the Presence of Different Concentrations of GSH in Ethanol−Water Solution

compound	τ_1 (ns)	τ_2 (ns)	χ^2 (%)	α_1 (%)	α_2 (%)	$\langle\tau\rangle$ (ns)
1a	4.01	−	1.125	100	0	4.01
1a−GSH[a]	3.31	5.17	1.096	82.92	17.08	3.76
1a−GSH[b]	3.64	5.23	1.067	22.49	77.51	4.96

[a] The concentration of GSH is 5.0×10^{-5} M. [b] The concentration of GSH is 1.0×10^{-3} M.

a result that is consistent with the predominance of the spiro-form in the absence of exogenous substrate. Figure 2B shows the typical emission spectra of **1a** toward different concentrations of GSH. In the presence of GSH, the 516 nm-band emission slightly decreases while a red-shifted, broad emission band centered at around 643 nm is observed, and its intensity increases with the GSH concentration. When the GSH concentration was ~1.5 mM, the emission maximum shifted to 643 nm. Further increase in GSH concentration leads to a slight increase in the emission intensity. The dynamic response range of the 643-nm band fluorescence emission is 0.01−5.0 mM GSH. We reasoned that the new emission of **1a** at long wavelength is due not only to an increase in concentration of the mero-form but also to GSH binding, which induces a conformational rigidity and subsequently changes the intramolecular charge transfer (ICT) between the phenolate oxygen and the electron-deficient quaternary nitrogen center.[43,44] The reduction in ICT (effectively unquenching) affords a dramatic enhanced and wavelength-shifted fluorescence as a function of the GSH concentration.

Fluorescence decay of the free **1a** in ethanol−water solution displays a single-exponential decay curve giving a satisfactory fit with a lifetime of ~4.0 ns.[40] Interestingly, in the presence of GSH in the ethanol−water solution, an additional component, with a long lifetime (~5.2 ns), was observed, and its relative abundance increased with an increase in GSH concentration (Table 2). We believe this long-lived species to be the **1a**−GSH complex. The multipoint interaction between the mero-form of **1a** and GSH may restrict the torsional dynamics of merocyanine, leading to a longer lifetime.

Because the formation of the opened mero-form of a spiropyran can be induced by H^+,[6,7] and considering that

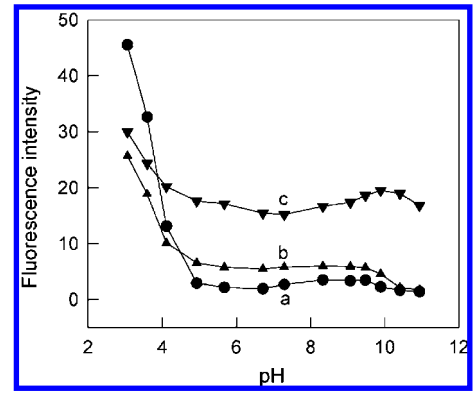

Figure 3. Fluorescence intensity−pH profiles for titrations of the ethanol−water solution of 2.5×10^{-5} M **1a** in the absence (a) and presence of 1.0×10^{-5} M (b) and 1.0×10^{-4} M (c) GSH. The excitation was at 446 nm, and emission was recorded at 643 nm.

the GSH complexation process requires the protonation of the phenolate oxygen, it is of importance to test whether the UV−visible absorption and fluorescence emission spectra changes of **1a** are due to the protonated form of the probe or to the GSH complex. Figure 3 depicts the fluorescence changes of **1a** at 643 nm as a function of pH in the absence and presence of GSH. The fluorescence signal of the free **1a** is higher in strongly acidic media than that in neutral or basic media, and the fluorescence intensity was hardly effected by H^+ or OH^- in the pH range of 4.5−10.0 (curve a). At a pH value below 5.0, **1a** converted to its protonated mero-form (HME^+), which in turn increases its long wavelength fluorescence emission. Curves b and c show the pH dependence of the **1a** fluorescence intensity for 1.0×10^{-5} and 1.0×10^{-4} M GSH, respectively. In the pH range of 4.5−10.0, the presence of GSH significantly increases the fluorescence intensity of the probe, and the fluorescence response of **1a** to GSH was nearly independent of pH between 5.3 and 8.4. Formation of protonated merocyanine of **1a** at pH below 5.3 or other ionic forms[45] of GSH at pH higher than 8.5 reduces the interaction between the host and guest and thus decrease in the long wavelength fluorescence emission of **1a**. These results suggest that at neutral or weakly basic conditions, the **1a** fluorescence enhancement is the result of the GSH complexation and not the probe protonation. In subsequent experiments, pH 7.2 was used as an optimum experimental condition.

(43) Aoki, S.; Kagata, D.; Shiro, M.; Takeda, K.; Kimura, E. *J. Am. Chem. Soc.* **2004**, *126*, 13377–13390.
(44) Badugu, R.; Lakowicz, J. R.; Geddes, C. D. *J. Am. Chem. Soc.* **2005**, *127*, 3635–3641.
(45) Yakobke, H. D.; Jeschkert, H. *Amino Acids, peptides and Proteins: An Introduction*; Akademie, Verlage: Berlin, 1977.

Complexation Characteristics of 1a and GSH. GSH-induced photophysical property changes of **1a** suggest that the spiropyran may be an appropriate optical probe for GSH sensing in aqueous solution. However, before it can be practically applied for a GSH assay, some key issues related to the complex, including the stoichiometry and association constant, the interaction mechanism, and influence of host−guest structure on the interaction, should be addressed.

First, what are the exact stoichiometry and association constant between the host and guest? To determine the stoichiometry and association constant of **1a** and GSH, the obtained fluorescent data as shown in Figure 2B were analyzed using eqs 1 and 2 (see Experimental Section). Nonlinear fitting with α as a function of GSH concentration shows the formation of a 1:1 GSH−**1a** complex and gives a corresponding association constant of $K = (7.52 \pm 1.83) \times 10^4$ M^{-1}.[40] The quantitative formation of a 1:1 complex between **1a** and GSH was further supported by cold-spray ionization time-of-flight mass spectrum (SI-TOFMS). The *m*/*z* formula $(M + H)^+$ of the free **1a** in ethanol was found to be 777.5130 (calculated: 777.5102) in its high-resolution mass spectrum. While in the SI-TOFMS of an ethanol−water solution containing 5.0×10^{-5} M **1a** and 5.0×10^{-5} M GSH, a new peak at $m/z = 1083.731$, which is assigned to $[\mathbf{1a} + GSH - 2H]^+$, is clearly observed.[40]

Second, how does **1a** interact with GSH? The interactions of **1a** with GSH were studied by ^{1}H NMR in ethanol-d_6 to provide some insights into the interaction mechanism. The ^{1}H NMR of free **1a** exhibits the typical ^{1}H signals of spiropyrans: two singlets at 1.15 and 1.27 ppm, assigned to the magnetically nonequivalent methyl protons and a singlet at 2.62 ppm, ascribed to the *N*-methyl protons of the indoline rings. When an equimolar amount of GSH (dissolved in D_2O) was added, the two singlets of the methyl protons coalesced into one singlet of ∼1.52, indicating they have become magnetically equivalent due to the planar structure of the fully conjugated merocyanine form. Also, the interaction with GSH caused a very pronounced downfield shift of the methylene protons of the linkage moiety (∼3.31 ppm) and methylene protons of piperazine moiety (∼2.18 ppm). As the vinyl protons are very sensitive indicators of ring-opening,[9a] the results primarily indicate GSH complexes with the opened mero-form of **1a**, and that the interaction may occur through the phenolate hydroxyl group and the ammonium moiety.

To test the effects of the phenolate oxygen of **1a** and positively charged ammonium of GSH on the complex, the fluorescence response of **1a** toward two dicarboxylates (succinate and isophthalate), two GSH derivatives (**3b** and **3c**, Chart 1), L-glutamate, and glutathione disulfide (GSSG) was examined, where **1a** was subjected to different concentrations of succinate, isophthalate, L-glutamate, **3b**, **3c**, and GSSG, separately, in 20% ethanol−water solution for an interaction time of 5 min. **1a** shows different fluorescence response behaviors to the charged complementary complexes: Succinate and isophthalate showed no effect on the fluorescence emission of **1a**, while slight increases in the emission intensity were observed from interaction with L-glutamate, the GSH ethyl monoester compound **3b**, or acylated compound **3c**, but the fluorescence intensity enhancement, F/F_0, is smaller than that of GSH, where F_0 and F are the **1a** fluorescence intensity at 643 nm in the absence and presence, respectively, of the analyte. The value of F/F_0 is 17.6 with 1.0 mM GSH, while it is only 4.3 with **3b** and 1.25 with succinate, respectively. It is worth noting that **1a** displays a similar fluorescence response toward GSSG ($F/F_0 = 10.7$) in comparison with GSH. By using curve fitting analysis, the association constants of **1a** with GSSG and L-glutamate were determined to be 3.47×10^4 M^{-1} and 9.85×10^2 M^{-1},[40] respectively, which is ca. 2.2- and 76- fold smaller than that of **1a** with GSH, whereas the binding constants of **1a** with succinate or isophthalate could not be determined because the corresponding change in fluorescence emission was too small. The optical selectivity coefficient, which was evaluated by comparing the association constant and the fluorescence signal change at 643 nm ($K \times R$),[46] are summarized in Table 3. From Table 3, the response of **1a** toward the substrates decreases in the order of GSH > GSSG > L-glutamate > **3b** > **3c** ≫ succinate > isophthalate. The target response selectivity combined with the GSH-induced ^{1}H NMR changes of **1a** suggest that both spiropyran moieties of **1a** participate in the formation of the complex with GSH via electrostatic interaction, which occurred through the ammonium of the indoline ring as well as the phenolate oxygens of the merocyanines, as schematically illustrated in Scheme 1B.

Table 3. Fluorescence Signal Changes at 643 nm (F/F_0), Association Constants (K), and Selectivity Coefficients of **1a** for Selected Dipolar Molecules

species	$(F/F_0)^a$	K (M^{-1})	response selectivity[b]
1a	1	−	−
1a + GSH	17.6	7.52×10^4	1
1a + GSSG	10.2	3.47×10^4	0.26
1a + L-glutamate	8.4	9.85×10^2	6.3×10^{-3}
1a + **3b**	4.3	192	6.3×10^{-4}
1a + **3c**	3.6	156	4.1×10^{-4}
1a + succinate	1.25	nd[c]	−
1a + isophthalate	1.46	nd[c]	−

[a] F_0 and F are the fluorescence intensity of **1a** at 643 nm in the absence and the presence of a target, respectively. The concentration of the target in each case was 1.0 mM. [b] Response selectivity = $(K_i(F/F_0)_i)/(K_{GSH}(F/F_0)_{GSH})$; the response for GSH was used as the standard. [c] The association constant could not be obtained because the fluorescence intensity changes of **1a** at 643 nm are too small in the presence of the analyte.

Finally, how does the structure of the host molecule affect the binding? To gain an insight into the effect of linkage length and spatial structure of the spiropyrans on the GSH complexation, the interactions of bis-spiropyran **1b** and mono-spiropyran **2**[9c] with GSH were further studied. **1b** contains two spiropyrans in its molecular backbone, but it cannot form a planar structure because of the orthogonal nature of the binol moiety. As shown in Figure 4A, addition of increased amounts of GSH to an ethanol−water solution of **1b** results in a slight increase in the UV−visible absorption at ∼450 nm. Upon excitation at the maximum absorption wavelength of 450 nm, **1b** fluoresces at 570 nm ($\Phi = 0.11$). Although the 570-nm emission band shifted to around 590 nm concomitant with a decrease in intensity from increased amounts of GSH, no new emission peak in the range of 600−700 nm could be observed (Figure 4B), indicating that there is no mero-component in the solution. By using the fluorescence intensity changes at 590 nm, the association constant of **1b** and GSH was determined to be $(3.21 \pm 1.06) \times 10^3$ M^{-1}. To compare the cooperative interaction to a similar noncooperative interaction, mono-spiropyran **2** was used. In 20% ethanol−water solution, **2** is red in color. Both the color and fluorescence of **2** hardly changed upon addition of 10 equiv of GSH. These results further demonstrate that the response of a

(46) Zhao, J. Z.; Fyles, T. M.; James, T. D. *Angew. Chem., Int. Ed.* **2004**, *43*, 3461–3464.

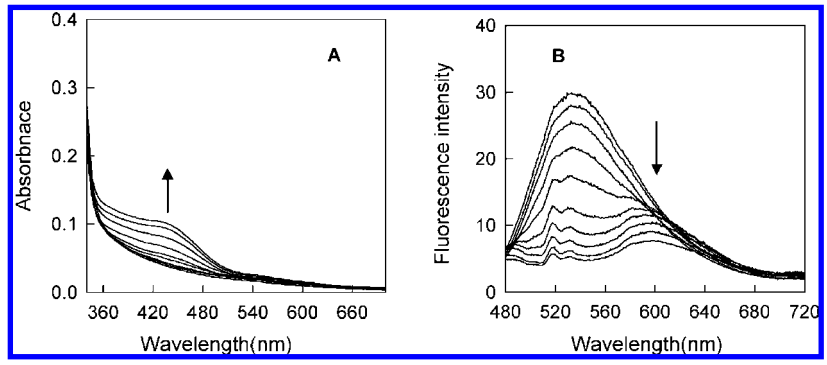

Figure 4. Absorption (A) and fluorescence emission (B, $\lambda_{ex} = 450$ nm) spectra of **1b** recorded in 20% ethanol−water solution in the presence of increasing amounts of GSH. Spectra shown are for GSH concentrations of 0, 0.025, 0.05, 0.1, 0.25, 0.5, 1.0, 2.5, 5.0, and 10.0 mM.

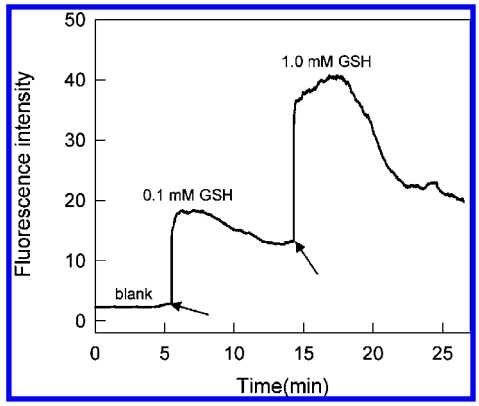

Figure 5. Time course of the interaction of **1a** (2.5×10^{-5} M) with different concentrations of GSH. Fluorescence intensity was recorded at 643 nm in 20% ethanol−water solution with an excitation wavelength of 446 nm. The transition between each regime is marked with an arrow.

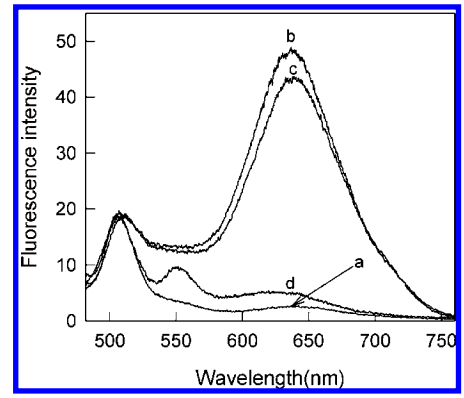

Figure 6. Fluorescence emission spectra of **1a** (2.5×10^{-5} M, room temperature, $\lambda_{ex} = 446$ nm) measured under different conditions: (a) emission of free **1a** in the ethanol aqueous solution, (b) emission after addition of 1.0 mM GSH, (c) emission of b after standing at room temperature for 6 h, and (d) emission of b after 15 min of irradiation with visible light (120-W tungsten flood lamp).

bis-spiropyran toward a zwitterionic molecule is a combination of multipoint electrostatic interactions and the structure complementarity of the host−guest.

GSH Binding Reversibility and Response Time. Another key feature of a sensing probe is response time and reversibility, i.e., on- and off-rates, in any given recognition process. In view of photoreversible structural conversion of the merocyanine complex, the real-time record of the interaction of **1a** with GSH was carried out using the 643-nm band fluorescence emission as a function of time. As shown in Figure 5, the formation of the GSH complex proceeds almost instantaneously as indicated by fluorescence enhancement. On the other hand, the response time depends on the change in concentration of GSH, as the time required to reach equilibrium increases with the GSH concentration. A stable reading was obtained within 2−4 min. It is worth noting, from Figure 5, that the fluorescence intensity of **1a** decreases with time after the interaction equilibrium, which implies that the GSH complex may undergo photodecomposition.

To test whether the fluorescence decrease of **1a** is a result of photoreversible structure conversion, two aliquots of the GSH complexes were prepared in ethanol−water solution. Figure 6 shows the fluorescence emission spectral changes of the aliquots without or with visible light irradiation. We were delighted to find that the GSH complex is thermally stable at room temperature within 6 h without visible light irradiation, while irradiation of the complex with visible light caused rapid dissociation of approximately 80% of the GSH complex (Figure 6, curve d). The regenerated spiropyran is fully functional and has been run through five cycles of GSH binding−release without detectable fatigue. This photocontrolled reversibility would facilitate the sensor application because additional reagent is not needed to release the free probe.

Probing Intracellular GSH. As discussed in the Introduction, GSH plays key roles in biological systems and serves many cellular functions. Therefore, the availability of a fluorescent probe that is able to detect cell GSH is very attractive.[26,30] Several features of **1a**, including the high affinity for GSH, favorable photophysical properties, and the moderate hydrophilicity, motivated us to explore its utility for in vivo studies to assess total cell GSH.

One basic requirement of an in vivo probe is its target selectivity over other competitive substrates. The fluorescence response of **1a** is highly selective for GSH over biologically relevant analytes (Figure 7). Alkali- and alkaline earth-metal ions in the 100 mM range, and transition metal ions, such as Cu^{2+}, Zn^{2+}, and Hg^{2+}, in the 0.1 mM range do not affect the fluorescence intensity of the probe, which indicates that these metal ions do not interfere with GSH detection.[40] We reasoned that the smaller response of **1a** toward Cu^{2+} in comparison with mono-spiropyran[9c,d] may be due to the difference in molecular backbones of the two spiropyrans. The opened form of the mono-spiropyran easily forms a 1:2 metal to ligand structure to stabilize the Cu^{2+} complex, while the spacer of **1a** between the two spiropyran units hampers the formation of the 1:2 metal to ligand structure. Inorganic and organic anions in the 1.0 mM

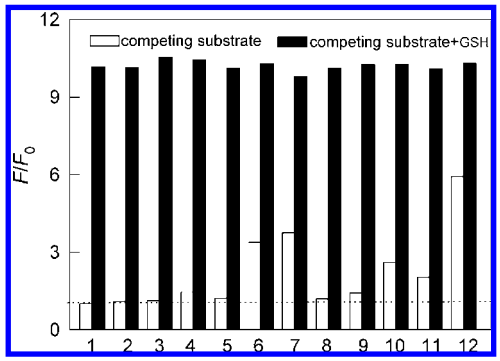

Figure 7. Fluorescence intensity change profiles of **1a** in the presence of selected substrates (BSA 0.1 mg/mL, Ca^{2+} 100 mM, others 0.1 mM). 1, blank; 2, Ca^{2+}; 3, Zn^{2+}; 4, Cu^{2+}; 5, Cl^{-}; 6, Glu; 7, Asp; 8, Cys; 9, BSA; 10, β-mercaptoethanol; 11, 3-mercaptopropanoic acid, and 12, GSSG. Bars represent the finial fluorescence response (F) over the initial emission (F_0). Excitation was at 446 nm, and emission was monitored at 643 nm.

range do not show any influence on the **1a** fluorescence emission. Amino acids, protein, and several thiol-containing analytes, such as β-mercaptoethanol and 3-mercaptopropanoic acid, at as high as 0.1 mM (higher than the typical intracellular concentration) produce only a very small increase in fluorescence intensity of the probe.

To further characterize the binding specificity of **1a** for GSH, competition experiments were conducted in which **1a** was first mixed with the competitive substrate, and GSH was then added to the mixture. As shown in Figure 7, no significant variations in the fluorescence intensity of **1a** were found in the presence of substrates other than GSH. These results clearly indicate that the approach is not only insensitive to other biologically related substrates but also selective toward GSH in the presence of other substrates. Although it is reasonable that GSSG induces an increase in the fluorescence intensity due to the structure similarity to GSH, when the large difference in the intracellular concentrations of GSSG and GSH is taken into account (in cells, the concentration of GSH is around 1−10 mM, whereas the concentration of GSSG is most likely in the micromolar range[23d]), the former does not cause substantial interference in the GSH determination. These results are important and helpful in validation of the method to meet the selectivity requirements of the GSH assay in physiological fields.

For application of a probe to living cells, a probe needs to be introduced into the cell interior. One method is to use a protecting group that is cleaved within the cell. In general, hydrophilic fluorescence probes, with the carboxylic acid protected by an acetoxymethyl group, or the phenol protected as an acetate ester, are introduced into the cell and are hydrolyzed by intracellular esterases.[47] Another method is to incorporate the probes into the membrane-permeable scaffold, such as using liposomes as delivery vehicles.[48] Because of the moderately high hydrophobicity of **1a**, we expected that the probe may diffuse across the cell membrane. To examine the membrane permeability of **1a**, **1b**, and **2**, their fluorescence anisotropies in cell environments were determined. The fluorescence anisotropy of a fluorophore reflects the molecule's ability to rotate in its microenvironment, which involves the

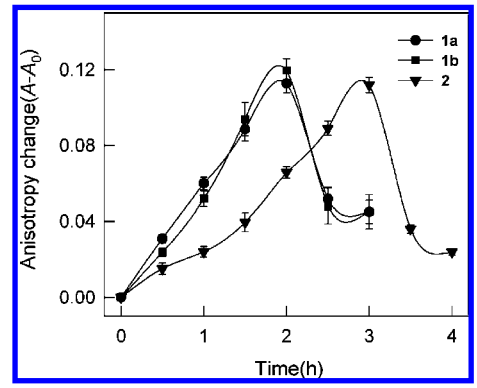

Figure 8. Comparison of time-dependent fluorescence anisotropy changes, ($A - A_0$), of **1a** (●), **1b** (■), and **2**(▼) in RPMI-1640 medium after incubating with human acute T cell leukemia. Here A_0 and A are the fluorescence anisotropies of the probes in cultured medium without or with human acute T cell leukemia. Fluorescence anisotropies were recorded at $\lambda_{ex}/\lambda_{em}$ = 462 nm/520 nm for **1a**, $\lambda_{ex}/\lambda_{em}$ = 450 nm/575 nm for **1b**, and $\lambda_{ex}/\lambda_{em}$ = 402 nm/440 nm for **2**, respectively.

viscosity of the solution, and the size and mass of the molecule to which the fluorophore is attached.[49,50] Therefore, this measurement can be used to judge whether a fluorophore is localized in the cell membrane or in solution. Spiropyrans are small molecules, so its binding with a cell will bring about a significant change in their molecular weights and, therefore, their rotational diffusion rates, resulting in detectable variations in their fluorescence anisotropy values.

We first measured the fluorescence anisotropies of **1a**, **1b**, and **2** in RPMI-1640 cultured medium containing 10% FBS (fetal bovine serum). As expected, no anisotropy could be observed. However, when the probes were added into cultured living cells and incubated over time, significant anisotropy changes could be observed. Figure 8 shows the anisotropy increase, ($A - A_0$), as a function of incubation time. Here A_0 and A are the fluorescence anisotropy of the probe in cultured medium without or with human acute T cell leukemia, respectively. The anisotropy changes were found to depend on the incubation time. In the case of **1a** or **1b**, maximal values of ($A - A_0$) were achieved within 2 h; a longer incubation time decreased its fluorescence anisotropy. As for **2**, the time to achieve maximum anisotropy is ~3 h. The anisotropy increases can be ascribed to the immobilization of part of the dyes inside the membranes or organelles. We reasoned that the anisotropy decreases, at times more than 2 h or 3 h, are due to distribution of the probes inside cells and interaction with the intracellular GSH to form the mero-GSH complex, as shown in Scheme 3.

We next assessed the ability of GSH to trigger the ring-opening of **1a** in living cells by confocal fluorescence microscopy. Jurkat cells were incubated in the absence and presence of **1a** in RPMI-1640 medium at 37 °C for 3 h and then washed three times with PBS. The cells were imaged on a FV500-IX81 confocal microscope with 458 nm laser line excitation and an emission BP600−620 nm filter. From Figure 9A, it could be seen that the TIB-152 cells had just a very slim intracellular spontaneous fluorescence without **1a.** When the cells were incubated with **1a** under the same conditions, strong fluorescence emission was detected from the cell interior (Figure 9B). These results indicate that **1a** efficiently

(47) Komatsu, K. K.; Kikuchi, K.; Kojima, H.; Urano, Y.; Nagano, T. *J. Am. Chem. Soc.* **2005**, *127*, 10197–10204.
(48) (a) Hettiarachchi, K.; Lee, A. P.; Zhang, S.; Feingold, S.; Dayton, P. A. *Biotechnol. Prog.* **2009**, *25*, 938–945. (b) Chen, M. L. *Adv. Drug Delivery Rev.* **2008**, *60*, 768–777.
(49) Schröder, G. F.; Alexiev, U.; Helmut Grubmüller, H. *Biophys. J.* **2005**, *89*, 3757–3770.
(50) Lakowicz, J. R. In *Principles of Fluorescence Spectroscopy*; 3rd ed.; Kluwer-Plenum Press: New York, 2006.

Scheme 3. Representation of the Spiropyran Transport across the Cell Membrane with Changes in Fluorescence Anisotropy

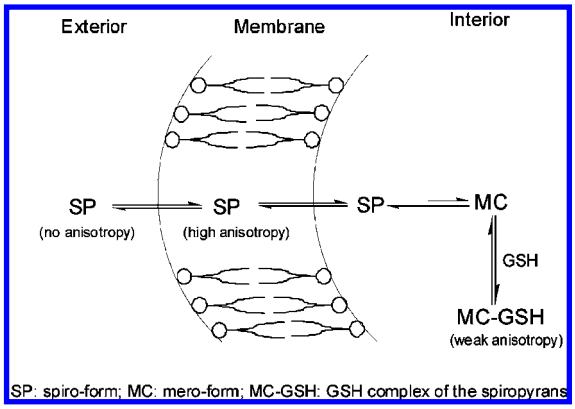

penetrated cell membranes and converted into highly fluorescent merocyanine, and the fluorescence is unlikely to be quenched by components of the biological milieu.

To confirm that the fluorescence from **1a** is the result of interaction of **1a** with endogenous GSH, a GSH-recognized oxidant (diamide)[51] was used. In this experiment, the cells were first treated with diamide for 2 h, washed three times, and then incubated with **1a** for 3 h and imaged as above. An obvious fluorescence decrease was observed due to a decrease in the GSH concentration. Because the 458 nm excitation line from the laser source converts the merocyanine into spiropyran, the red fluorescence from **1a** becomes weaker with increasing exposure time so that by 30 s the intensity was severely attenuated (not shown). Finally, bright-field transmission measurement confirms that the spiropyran probe has low toxicity[52−54] and cells are viable throughout the imaging studies. Taken together, these results demonstrate that at room temperature, **1a** could readily internalize into the cytoplasm of the cell with visible wavelength excitation and emission energies and can be accumulated intensively into the cells (i.e., cytoplasm) to show a level of intracellular GSH.

Conclusion

We have developed the first spiropyran ligands for dipolar molecules and applied them to in vivo GSH fluorescent probes. Interaction between the zwitterionic merocyanine of a spiropyran and a charged complementary molecule provides a potential approach for neutral molecule sensing. Nevertheless, no practical spiropyran probe for these analytes has been available. We designed and synthesized bis-spiropyrans with an off/on fluorescence switched by GSH complexation based on multipoint electrostatic interactions and structure complementarity of the host−guest. Although many molecular probes have been utilized for detection of GSH,[25−38] **1a** is markedly superior to known GSH probes, especially for its ability to detect GSH without interference from other thiol-containing components, and should be suitable for high-throughput screening. Moreover, the comparatively good intracellular delivery (without application of any other transfection technique) of **1a** indicates it can be highly concentrated into the cells (i.e., cytoplasm) and is available for imaging GSH in living cells. These results demonstrate that **1a** may be useful in a wide range of biological and microscopic applications such as in vivo utilization as a GSH marker to visualize the level of intracellular GSH.

Experimental Section

Materials and Apparatus. All inorganic reagents and amino acid derivatives were of analytical reagent grade and were obtained from Aldrich or Sigma. Spiropyran **2** was previously synthesized in our laboratory.[9c] Synthesis and characterization of compounds **1a**, **1b**, and **3c** are presented in the Supporting Information.[40] The stock solutions of 0.05 M GSH and amino acids were prepared by dissolving the materials in water. Working solutions were prepared by successive dilution of the stock solution with phosphate-buffered saline (PBS, pH 7.2). All stock solutions of metal ions were prepared from analytical grade nitrate salts and were dissolved in doubly distilled water. The work solutions of metals were obtained by series dilution of the stock solutions with PBS. The stock solutions of 1.0×10^{-3} M **1a**, **1b**, and **2** were obtained by dissolving the compounds in ethanol, respectively.

Jurkat cell lines (TIB-152, human acute T cell leukemia) were grown in pH 7.2 RPMI 1640 medium (ATCC) supplemented with 10% FBS (fetal bovine serum) (heat inactivated, GIBCO) and 100 IU/mL penicillin−streptomycin (Cellgro) at 37 °C in a CO_2 incubator. Cells were washed before and after incubation with the washing buffer (4.5 g/L glucose and 5 mM $MgCl_2$ in Dulbecco's PBS with calcium chloride and magnesium chloride (Sigma)).

Proton magnetic resonance spectra were recorded at 400 MHz and carbon spectra were recorded at 100 MHz on an Invoa-400 (Invoa 400) spectrometer with tetramethylsilane (TMS) as the internal standard. *J* values were given in hertz. High-resolution mass spectra were obtained on a Q-Star Pulsar I (Applied Biosystem/PE Sciex). The cold-spray ionization time-of-flight mass spectra (CSI-TOFMS) were acquired using an AccuTOFCS mass spectrometer (JMS-T100CS, Tokyo, Japan). UV−visible absorption spectra were recorded on a Hitachi U-4100 UV/vis spectrophotometer (Kyoto, Japan). Fluorescence emission spectra were recorded on a Hitachi F-4500 fluorescence spectrofluorometer (Kyoto, Japan). The fluorescence lifetime was measured with an Edinburgh Instruments FLS 920 (UK) luminescence spectrophotometer. Fluorescence micrographs were collected on an FV500-IX81 confocal microscope (Olympus America Inc., Melville, NY) with a 60× oil immersion objective (NA = 1.40, Olympus, Melville, NY).

Fluorescent Titrations and Association Constant. Fluorescence titrations were carried out in 20% ethanol−water (v/v) solution at pH 7.2 by adding a few microliters of a stock solution of the analytes to 2.0 mL of 5.0×10^{-5} M **1a** with a quartz cell (1.0×1.0 cm^2 cross-section). The addition was limited to 100 μL so that the volume change was insignificant. The fluorescence emission spectra were obtained by exciting at the maximal absorption wavelength as determined by UV titrations. The obtained data of the intensity of **1a** at 643 nm were analyzed for association constant *K* using the relationship established in the formation of *n*:*m* ligand (L) to guest (GSH, G) complex.[55]

$$[G]^m = \frac{1}{nK} \times \frac{1}{[L]_T^{n-1}} \times \frac{1-\alpha}{\alpha^n} \quad (1)$$

$$\frac{1-\alpha}{\alpha} = \frac{F - F_{min}}{F_{max} - F} \quad (2)$$

where [G] and [L] denote the free concentration of GSH and ligand **1a**, respectively, α is the ratio between the free ligand concentration, [L], and the initial concentration of the ligand, L_T. *F* is the

(51) Becker, P. S.; Cohen, C. M.; Lux, S. E. *J. Bio. Chem.* **1986**, *261*, 4620–4628.
(52) Zhu, L. Y.; Wu, W. W.; Zhu, M. Q.; Han, J. J.; Hurst, J. K.; Li, A. D. Q. *J. Am. Chem. Soc.* **2007**, *129*, 3524–3526.
(53) Hu, D. H.; Tian, Z. Y.; Wu, W. W.; Wan, W.; Li, A. D. Q. *J. Am. Chem. Soc.* **2008**, *130*, 15279–15281.
(54) Tian, Z. Y.; Wu, W. W.; Wan, W.; Li, A. D. Q. *J. Am. Chem. Soc.* **2009**, *131*, 4245–4252.
(55) Yang, R. H.; Wang, K. M.; Long, L. P.; Xiao, D.; Yang, X. H. *Anal. Chem.* **2002**, *74*, 1088–1096.

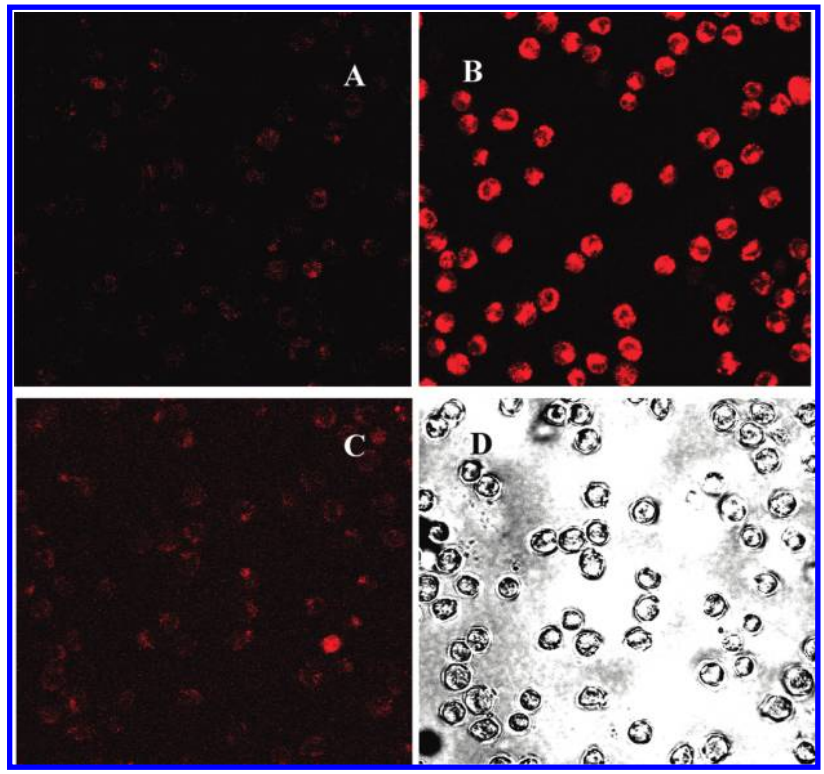

Figure 9. Confocal microscope images of human acute T cell leukemia (A) without spiropyran, (B) incubated with 100 μM **1a** for 3 h, (C) incubated with 1.0 mM diamide for 2 h and then 100 μM **1a** for 3 h, and (D) bright-field transmission image of C.

fluorescence intensity of **1a** at 643 nm in the presence of different concentrations of GSH, and F_{min} and F_{max} are the limiting values of F at zero GSH concentration and at final (plateau) GSH concentration, respectively. The experimental data were fitted to eq 2 by changing the ratio of m to n and adjusting the association constant.

Determination of Fluorescence Quantum Yields (Φ_F). For measurement of the quantum yields of **1a** and **1b**, the ethanol solution of the compounds was adjusted to an absorbance of ~0.05. The emission spectra were recorded using the maximal excitation wavelengths, and the integrated areas of the fluorescence-corrected spectra were measured. The quantum yields were then calculated by comparison with *meso*-tetraphenylporphyrin (TPP) as reference using the following equation:[56]

$$\Phi_F = \frac{I}{I_R} \times \frac{A_R}{A} \times \left(\frac{n}{n_R}\right)^2 \times \Phi_R \qquad (3)$$

where Φ_F is the quantum yield of **1a** or **1b**, I is the integrated area under the fluorescence spectra, A is the absorbance, n is the refractive index of the solvent, and R refers to the reference fluorophore, TPP. $\Phi_R = 0.11$ in cyclohexane was used as the reference quantum yield.[57]

Fluorescence Lifetime Measurements. Fluorescence lifetimes of **1a**, **1b**, and their GSH complexes were calculated from time-resolved luminescence intensity decays on an Edinburgh Instruments FLS 920 luminescence spectrophotometer in the time-correlated single photon counting mode. All experiments were performed using excitation and emission slits with a nominal band-pass of 5.0 nm. The data stored in a multichannel analyzer was routinely transferred to a computer for analysis. Intensity decay curves so obtained were fitted as a sum of exponential terms[49]

$$F(t) = \sum_i \alpha_i \exp(-t/\tau_i) \qquad (4)$$

where α_i is a pre-exponential factor representing the fractional contribution to the time-resolved decay of the component with a lifetime τ_i. The decay parameters were recovered using a nonlinear least-squares interative fitting procedure.[58] A fit was considered acceptable when plots of the weighted residuals and the autocorrelation function showed random deviation about zero with a minimum χ^2 value not more than 1.5. Mean (average) lifetimes $\langle\tau\rangle$ for biexponential decays of luminescence were calculated from the decay times and pre-exponential factors using the following equation[49]

$$\langle\tau\rangle = \frac{\alpha_1\tau_1^2 + \alpha_2\tau_2^2}{\alpha_1\tau_1 + \alpha_2\tau_2} \qquad (5)$$

Confocal Imaging. All cellular fluorescent images were collected on an FV500-IX81 confocal microscope. The excitation wavelength was 458 nm laser line, and an emission BP600−620 nm filter was used. For the cell uptake experiment, 5×10^5 cells were first washed with 500 μL washing buffer at 4 °C once and then incubated with 10 μM **1a** in RPMI-1640 medium at 37 °C for 3 h. Internalization was stopped by placing the cells on ice immediately after the incubation, and cells were washed three times with 500 μL of washing buffer at 4 °C. Before the imaging, 100 μL of cell suspension was dropped on the poly-D-lysine-coated 35 mm glass bottom dishes (Mat Tek Corp), and 3 min was allowed for the cells

(56) (a) Arimori, S.; Bell, M. L.; Oh, C. S.; Frimat, K. A.; James, T. D. *J. Chem. Soc., Perkin Trans. 1* **2002**, 803–808. (b) Onoda, M.; Uchiyama, S.; Stana, T.; Imai, K. *Anal. Chem.* **2002**, *74*, 4089–4096.

(57) (a) Seybold, P. G.; Gouterman, M. *J. Mol. Spectrosc.* **1969**, *31*, 1–13. (b) Quimby, D. J.; Longo, F. R. *J. Am. Chem. Soc.* **1975**, *97*, 5111–5117.

(58) Bevington, P. R. In *Data Reduction and Error Analysis for the Physical Sciences*; McGraw-Hill: New York, 1969.

to settle. All the data were collected three times and analyzed using Fluoview analysis software. To confirm that the fluorescence from **1a** is a result of the GSH complex, a GSH-recognized reagent (diamide) was used. In this experiment, the cells were treated with diamide for 2 h, washed three times, and then incubated with 10 μM **1a** for 3 h and imaged as above.

Acknowledgment. The work was supported by the National Outstanding Youth Foundation of China (20525518), National Natural Foundation of China (20775005), and Hong Kong Research Grant Council (HKBU 200407).

Supporting Information Available: Synthesis and characteristics of **1a** and **1b**, fluorescence response of **1a** toward different targets, pH effect, association constants, fluorescence decay curves, and ^{1}H NMR, ^{13}C NMR, and mass spectra. This material is available free of charge via the Internet at http://pubs.acs.org.

JA908215T